Tyrosinase-Generated Quinones Induce Covalent Modification, Unfolding, and Aggregation of Human Holo-Myoglobin

Alessandro Granata, Raffaella Roncone, Enrico Monzani, and Luigi Casella*

Dipartimento di Chimica Generale, Università di Pavia, Via Taramelli 12, 27100 Pavia, Italy

Received April 13, 2007; Revised Manuscript Received July 11, 2007

The present study describes the pattern of protein modification undergone by human holo-myoglobin by reactive fluoroquinones enzymatically produced by oxidation of 3-fluorophenol in mild conditions (pH 7.4, 25 °C). The fluoroquinones react with a number of histidine residues. Surface residues H24, H36, H48, and H82 and the heme distal histidine H64 were all found to be modified to a significant extent. In contrast, cysteine C110 is not appreciably affected, possibly because it is not accessible to the fluoroquinones. The sites of protein modification were assessed by mass spectrometry analysis of the peptide fragments resulting from controlled proteolysis of the apoprotein. As a consequence of the reaction with quinones, the globular structure of myoglobin becomes more prone to denaturation by the partial loss of its secondary structure. As a more intriguing consequence, the fluoroquinones promote the formation of structured aggregates of moderate size that lack the typical morphology of fibrillar structures.

Introduction

Reactive oxygen (ROS) and nitrogen species (RNS) are able to react with a variety of cellular components, resulting in detrimental effects on their function. These species include both free radicals, such as superoxide anion, nitrogen monoxide, nitrogen dioxide, and hydroxyl radical, and other molecular species, such as hydrogen peroxide, dinitrogen trioxide, and peroxynitrite. ROS and RNS have been implicated in many disease states, where they typically induce oxidation and nitration of proteins; important examples include the pathogenic mechanisms of neurodegenerative diseases[1−3] as well as cardiovascular disfunctions.[4] A large body of evidence, in particular, shows that both oxidized[5−10] and nitrated proteins[11−16] are associated with neuronal disorders and age-related pathologies, such as Parkinson's disease and Alzheimer's disease.[3,17] In fact, these modifications can induce protein misfolding and aggregation, including filamentous inclusions with fibrillar characteristics; although it is still not known whether these species are the primary causes of the pathologies. Actually, it has been shown that soluble prefibrillar oligomers may be more toxic than the fibrils themselves, which can be sequestered in inclusion bodies.[18,19]

An additional source of damage of cellular components that is common to neurons of the substantia nigra pars compacta and the locus coeruleus of the brain stem is dopamine, which can readily undergo oxidation reactions generating ROS as well as the reactive dopamine quinone (DAQ).[20,21] The presence of insoluble intracellular deposits of neuromelanin in these brain regions indicates that spontaneous or induced oxidation of dopamine and other neuronal catechols occurs in vivo.[22] It is assumed that dopamine-generated ROS give rise to oxidative modification or breakdown of the protein targets (or other cellular components).[23−26] However, reactive DAQ species can readily form covalent adducts with proteins or other nucleophilic molecules, and indeed several neuronal proteins, including α-synuclein,[27] the human dopamine transporter,[28] tyrosine hydroxylase,[29] and parkin,[30] have been recently found to form DAQ adducts. Formation of these protein−DAQ adducts is likely to produce structural effects on the target proteins that could lead to impairment of their functions. For instance, DAQ modification of α-synuclein has been recently shown to produce sodium dodecyl sulfate (SDS)-stable oligomers and prevent the formation of insoluble amyloidogenic fibrils.[31,32] Effects similar to those induced by dopamine can be ascribed to L-3,4-dihydroxyphenylalanine (L-Dopa),[31,33−35] the precursor of dopamine and also used as a therapeutic agent for the symptomatic relief of Parkinson's disease, and other biogenic catecholamines.

In general, the pattern of DAQ modification of the target proteins is not known, though this knowledge would be extremely important to clarify whether the effects produced are site-specific. It is often assumed that the reaction occurs at cysteine residues, because the thiol group is highly reactive toward quinone residues,[36] but DAQ reactions can also occur at other residues, as it must be evident, for instance, for α-synuclein, which contains no cysteine. In the present study, we describe the pattern of quinone modification undergone by human (holo) myoglobin (hMb) and the structural effects thereby produced. To identify the sites of protein modification we found it particularly useful to use 3-fluorophenol as the source of the quinone (fQ), the latter species being generated by reaction with tyrosinase. Fluorophenols are "slow" substrates of tyrosinase, and we have previously shown that with these substrates it is possible to control the enzymatic reaction,[37] slowing down the formation of oligomeric and insoluble polymeric melanin pigments,[38] which occurs when substrates such as dopamine and L-Dopa are used. For the objective of the present study, the competitive melanization reaction represents a serious problem because the insoluble pigment can conglomerate the quinone-derivatized protein, thereby complicating the analysis of the modification sites. The presence of a fluorine atom in the fQ-modified protein is also useful in the analysis of the target reaction sites. Regarding the use of tyrosinase as fQ or DAQ inducer, although its role in the central nervous system is still unclear, its activity can be beneficial against the neurotoxicity induced by excess dopamine through the formation of neu-

* Author to whom correspondence should be addressed. Fax: +39 0382 528544. E-mail: bioinorg@unipv.it.

10.1021/bm070409h CCC: $37.00
Published on Web 09/21/2007

romelanin. In fact, tyrosinase mRNA appears to be expressed in human substantia nigra.[39] In addition to tyrosinase, other oxidative enzymes, such as peroxidase[40] and prostaglandin H synthase,[41] or even activated microglia[42] can easily generate DAQ from dopamine. An important result of the present investigation is that fQ-modified holo-hMb undergoes oligomerization to structured protofibrillar aggregates. Previously, amyloid fibrils of Mb (from horse skeletal muscle) were only obtained from the apoprotein under harsh conditions (heating to 65 °C for 24 h at pH 9.0),[43,44] whereas the fQ modification studied here is capable of disrupting the compact globular structure of the holo protein under physiological conditions.

Materials and Methods

Materials. Human myoglobin (RZ ≥ 3.0) was expressed and purified according to the method previously reported by us.[45] *Agaricus bisporus* tyrosinase (3960 units/mg) was obtained from Sigma and purified according to Duckworth and Coleman's procedure.[46] 3-Fluorophenol, dopamine, nitroblue tetrazolium, Congo Red, and trypsin from bovine pancreas (12 900 units/mg) were obtained from Sigma-Aldrich. RapiGest SF was obtained from Waters. All of the other chemicals were of analytical grade and used as received.

Reverse-Phase High-Performance Liquid Chromatography Analysis. The reaction between mushroom tyrosinase, 3-fluorophenol, and hMb was performed in 10 mM phosphate buffer, pH 7.4, at 25 °C. The reaction was started by adding mushroom tyrosinase (final concentration of 10 nM) to the solution containing 0.028 mM hMb and 0.42 mM 3-fluorophenol (molar ratio 1:15) to a final volume of 2 mL. After reaction times of 0, 4, 8, 24, and 48 h, a small amount (250 μL) of the reaction mixture was passed through a PD-10 column (Sephadex G-25 M, Amersham Biosciences) previously equilibrated with 10 mM phosphate buffer, pH 7.4. Separation of hMb−fQ derivatives from unreacted fluorophenol and other oligomeric quinone products occurred by elution with the same buffer. The first reddish band was collected, concentrated using a Microcon centrifugal filter divice (Microcon YM-10, Millipore), and analyzed by high-performance liquid chromatography (HPLC; Jasco MD-1510) using a Supelco reverse-phase C8 column (23 mm × 4.6 mm). Elution was carried out using 0.1% trifluoroacetic acid (TFA) in distilled water (solvent A) and 0.1% TFA in acetonitrile (solvent B) at a flow rate of 1 mL/min. Elution started with 65% solvent A for 10 min, decreasing to 63% A over 5 min, and 60% A over another 5 min. Solvent A was further decreased to 57% over 10 min and 40% over 25 min. During an additional 10 min the eluting solvent decreased to 0% A, remained stable for 5 min, and finally returned to 65% A over 5 min. Spectrophotometric detection of the eluates was performed in the range of 200−650 nm.

Two-Dimensional and SDS-PAGE Analysis. Reaction conditions between tyrosinase, 3-fluorophenol, and hMb were the same as those described in the previous section. Only the sample reacted for 4 h was passed through the PD-10 column, its volume reduced to about 100 μL by centrifugation at 10 000 rpm using Microcon YM-10 (Millipore), and finally analyzed. Native and modified hMb solutions were diluted 1:2 with a solution containing 8 M urea, 4% (w/v) 3-[(3-cholamidopropyl)dimethylammonio]-1-propanesulfonate (CHAPS), and 40 mM Tris. After centrifugation, 125 μL of each sample containing about 25 μg of protein was loaded onto the gel. Two-dimensional polyacrylamide gel electrophoresis (PAGE) was performed using the immobilized pH gradient system.[47] The first dimension, isoelectric focusing, was performed on laboratory-made gels, cast on Gel-Bond (Amersham Biosciences) with a 4.0−10.0 nonlinear immobilized pH gradient obtained with acrylamide buffer solutions (Fluka), and the separation was run in the Multiphor II horizontal system (Amersham Biosciences).

The gel strips were then placed on top of vertical 20% gels, and the second dimension run was performed using a Mini PROTEAN II cell (BioRad). SDS-PAGE (20% gel) was performed by the method of Laemmli,[48] and the gel was stained with Coomassie Blue.

Protein Blotting Analysis. Reaction conditions were the same as those described for the reverse-phase HPLC experiments. The reaction was started by adding mushroom tyrosinase (final concentration 50 nM) to the solution containing 0.044 mM hMb and 0.66 mM 3-fluorophenol (molar ratio 1:15) to a final volume of 1 mL. After a reaction time of 4 h, the samples were diluted with sample buffer and heated for 5 min at 95 °C. Samples were then loaded and electrophoresed in a 15% PAGE gel. Electrophoretic transfer of proteins from the polyacrylamide gel onto nitrocellulose paper was performed at 100 V for 1 h at 10 °C using a pH 8.3 blotting buffer containing 5 mM Tris, 38 mM glycine, and 20% methanol. Proteins were stained with Ponceau S (0.1% in 5% acetic acid), resulting in a red stain; the nitrocellulose paper was then washed four times with Milli-Q water. Quinoproteins were detected by staining with nitroblue tetrazolium (NBT; 0.24 mM in 2 M potassium glycinate, pH 10). The nitrocellulose paper was immersed in the glycinate/NBT solution for 45 min in the dark, resulting in a blue-purple stain of quinoprotein bands while the already stained, unmodified proteins remained red.

Mass Spectrometry Analysis. A portion of the sample utilized for the two-dimensional and SDS-PAGE analysis was analyzed by mass spectrometry (MS). MS data were obtained using a LCQ DECA ion trap mass spectrometer equipped with an electrospray ionization (ESI) ion source and controlled by Xcalibur software, version 1.3 (ThermoFinnigan, San Jose, CA). ESI experiments were carried out in positive ion mode under the following constant instrumental conditions: 4.5 kV source voltage, 15 V capillary voltage, 250 °C capillary temperature, 15 V tube lens voltage.

Analysis of Protein Fragments. The modifications induced on hMb by 3-fluorophenol in the presence of tyrosinase were studied in 10 mM phosphate buffer, pH 7.4, at 25 °C by mixing 0.10 mM hMb and 1.5 mM 3-fluorophenol in a final volume of 1 mL. The reaction was started by the addition of mushroom tyrosinase (final concentration of 50 nM). After 4 h of reaction time, the solution was passed through a PD-10 column, eluted with the same buffer, and collected. For the analysis of the protein fragments, the protein sample was transformed into the apoprotein by the standard hydrochloric acid/2-butanone method[49] and subsequently hydrolyzed by trypsin. To enhance in-solution enzymatic digestion of proteins, the RapiGest SF reagent was used. The sample volume was reduced to 750 μL by centrifugation at 10 000 rpm using Microcon YM-10 (Millipore) and incubated at 37 °C for 2 min with the RapiGest SF reagent. (The RapiGest SF concentration was 0.1% (w/v) after mixing with the protein solution.) Digestion was then performed by the addition of trypsin (trypsin/hMb 1:40 (w/w)) at 37 °C for 1 h in 10 mM phosphate buffer, pH 7.4. The sample was then treated with HCl (final HCl concentration of 40 mM) and incubated at 37 °C for 45 min. The acid-treated hMb was centrifuged at 13 000 rpm for 10 min and finally analyzed by HPLC-MS/MS.

The modification of apo-hMb by fQ species was obtained by treatment of the apoprotein (0.1 mM), obtained by the standard hydrochloric acid/2-butanone method,[49] with 1.5 mM 3-fluorophenol in the presence of tyrosinase (50 nM) in 1 mL of 10 mM phosphate buffer, pH 7.4, at 25 °C. After 4 h of reaction time, the solution was passed through a PD-10 column, eluted with the same buffer, and collected. Tryptic hydrolysis and the preparation of the sample for HPLC-MS/MS analysis was performed as above.

For the HPLC-ESI-MS/MS analysis, the system was run in automated LC-MS/MS mode using a Surveyor HPLC system (ThermoFinnigan, San Jose, CA) equipped with a Simmetry300 C18 column, 3.5 μm, 2.1 mm × 100 mm (Waters Milford, MA). The elution was performed with a 0−55% linear 65 min gradient using 0.1% TFA in water as solvent A and 0.1% TFA in acetonitrile as solvent B. MS/MS spectra obtained by collision-induced dissociation (CID) were performed with an isolation width of 3 Th (m/z); the activation amplitude was around 35% of the ejection radio frequency amplitude that corresponds to 1.58 V. For the analysis of protein fragments derived from hMb−fQ adducts, the mass spectrometer was set such that one full MS scan was followed by zoom scan and MS/MS scan on the most intense ion

from the MS spectrum. The acquired MS/MS spectra were automatically searched against a database for human proteins (human.fasta) using the SEQUEST algorithm to identify the modified residues. This algorithm has been incorporated into Bioworks 3.0 (ThermoFinnigan, San Jose, CA). For the analysis of protein fragments of modified hMb−fQ adducts, the mass spectrometer was set in MS/MS mode of parent bicharged ions 841.9 (mass of 1683.8 amu), 998.3 (mass of 1994.6 amu), 1180.1 (mass of 2358.3 amu), 1333.1 (mass of 2664.2 amu), and 1815.7 (mass of 363.4 amu).

Circular Dichroism. The reaction conditions for the modification of hMb by 3-fluorophenol in the presence of tyrosinase were the same as those described above. Reaction mixtures were analyzed after 0, 2, and 4 h reaction times and terminated, at each time, by loading a convenient aliquot (300 μL) on a PD-10 column previously equilibrated with 10 mM phosphate buffer, pH 7.4. The first reddish band was collected, and the hMb concentration was determined by UV−vis spectra (assuming $\epsilon_{410} = 150\ \mathrm{mM^{-1}\ cm^{-1}}$ as for wild-type met-hMb). Circular dichroism (CD) spectra of each sample were measured with a JASCO J-715 spectropolarimeter. The spectra were recorded in the 190−240 nm wavelength range with a 50 nm/min scanning speed. To reduce the signal-to-noise ratio 16 scans were accumulated. The path length was 0.1 cm. The data were converted to residual molecular ellipticity and analyzed using the Jasco Secondary Structure Estimation software (version 1.00.00) to evaluate the secondary structure content of fQ-modified hMb.

Guanidine Hydrochloride Denaturation Assay. The stability to denaturation of the hMb−fQ derivatives was determined by monitoring the absorbance variation of the Soret band of the protein (about 6 μM) upon addition of increasing amounts of a 8 M guanidine hydrochloride (Gdn-HCl) solution (0−3.0 M) to the protein solution in 10 mM phosphate buffer, pH 7.4. Reaction conditions between tyrosinase, 3-fluorophenol, and hMb to generate fQ-modified hMb were the same as those described in the previous section. Similarly to reverse-phase HPLC analysis, the Gdn-HCl denaturation assay was performed after reaction times of 0, 4, 8, 24, and 48 h. The curves of absorbance of the Soret band versus denaturant concentration were fitted with the following equation[50]

$$\frac{(A_i - A_U)}{(A_N - A_U)} = \frac{1}{1 + \exp\{([D] - [D_0])/d'\}} \qquad (1)$$

where A_i is the absorbance maximum (408 nm) of the Soret band at each denaturant concentration, A_N and A_U are the absorbances of the folded and unfolded forms, respectively, [D] is the Gdn-HCl concentration (M), [D_0] is the Gdn-HCl concentration at 50% unfolding of the protein, and d' is a constant connected to the shape of the sigmoid curve. Data were normalized so that the absorbance value of 1.0 corresponds to the completely folded state of the proteins and corrected for dilution by Gdn-HCl addition.

At each denaturant concentration, the Gibbs energy of unfolding, ΔG°_{obs}, was calculated, assuming the system to be in an equilibrium state, through the equation[50]

$$\Delta G^\circ_{obs} = -RT \ln \frac{(A_N - A_i)}{(A_i - A_U)} \qquad (2)$$

where A_i is the absorbance at each denaturant concentration. From the linear plot of ΔG°_{obs} versus [Gdn-HCl], the Gibbs energy change, ΔG°_{N-U} (kcal/mol), for the conversion of native to unfolded protein in the absence of denaturating agent, and the $-m$ parameter (kcal $\mathrm{mol^{-1}\ M^{-1}}$), related to the solvent-exposed surface area of the protein, were determined.

Congo Red Spectroscopic Assay. A solution of Congo Red (7 mg/mL) in 10 mM phosphate buffer, 150 mM NaCl, pH 7.4, was prepared and filtered through a 0.2 μm syringe filter immediately prior to use. A diluted solution of Congo Red was prepared by adding 10 μL of the mother Congo Red solution to 2 mL of 10 mM phosphate buffer, pH 7.4. Reaction conditions between mushroom tyrosinase, 3-fluorophenol, and hMb were the same as those described in the reverse-phase HPLC section. After 24 and 48 h reaction times, 500 μL of the reaction solution was added to the diluted Congo Red solution. The mixture was magnetically stirred for a few seconds at room temperature, and then a blank UV−vis trace between 400 and 700 nm was recorded. The solution was incubated for 30 min at room temperature, and a red precipitate was formed. After 30 min, the solution spectrum between 400 and 700 nm was recorded, and a band at 540 nm was observed.

To test for possible interference by the other species present in the reaction mixture, four blanks were performed. A Congo Red spectrophotometer assay described previously was applied to four solutions containing, respectively: (1) hMb (0.028 mM); (2) tyrosinase (50 nM); (3) 3-fluorophenol (0.42 mM) and tyrosinase (50 nM); (4) hMb (0.028 mM) and tyrosinase (50 nM). After 30 min of incubation time, the blank solution spectrum between 400 and 700 nm was recorded, and a band at 540 nm was not observed.

Congo Red Birefringence Assay.[51,52] A staining solution of Congo Red in 80% EtOH/20% double distilled water and saturated NaCl was prepared. This solution was stirred for a few minutes and then filtered to obtain the final working solution. Reaction conditions between mushroom tyrosinase, 3-fluorophenol, and hMb were the same as those described in the reverse-phase HPLC section. After 24 and 48 h reaction times, a few microliters of the reaction solution were added to 300 μL of the staining solution on a glass microscope slide. The stained sample was examined using polarized light microscopy.

Fluorine NMR Experiments. ^{19}F NMR measurements were performed on a Bruker AVANCE spectrometer operating at a proton Larmor frequency of 400.13 MHz. The reaction solution contained 2.0 mM hMb, 30 mM 3-fluorophenol, and 5.0 mM CF_3CH_2OH (used as an internal standard) in deuterated sodium phosphate buffer, pD 7.4, 25 °C. (The small deuterium effect on pH was neglected.) The reaction was started by the addition of tyrosinase dissolved in the same deuterated buffer (50 nM). The blank experiment was carried out in the same conditions as above but without hMb. Both reactions were followed for 1 h, by recording the ^{19}F NMR signal every 10 min. The amount of fluoride generated at various times by the reaction was determinated by using the integral of the signal of the internal standard CF_3CH_2OH as a reference and then normalizing the integral of the fluoride signal.

Transmission Electron Microscopy. The reaction conditions for the modification of hMb by 3-fluorophenol in the presence of tyrosinase were the same as those described in the reverse-phase HPLC experiments. After 8, 24, and 48 h reaction times, the samples were stained with 1% uranyl acetate. Specimens were transferred to thin carbon films supported by a 400 mesh copper grid and pretreated with glow discharge. Unbuffered 1% uranyl acetate was used as a negative stain. Observations were made using a Phillips/FEI Technai 12 electron microscope, and transmission electron microscopy (TEM) images were recorded using TIA 2024 × 2024 digital camera.

Results

Formation of hMb−fQ Adducts. Upon reaction of hMb with tyrosinase and 3-fluorophenol, the solution progressively turns to a more intense reddish color, which is indicative of the formation of quinone oligomers and their possible reaction with the protein. The derivatization of hMb was studied in 10 mM phosphate buffer, pH 7.4, at 25 °C, using a standard protocol. In all of the experiments, the molar ratio between 3-fluorophenol and hMb (28−100 μM) was 15:1, while the tyrosinase concentration was 10−50 nM. After the reaction, separation of the hMb derivatives from unreacted fluorophenol and unbound fQ oligomerization products was carried out using a PD-10 column by elution with the same phosphate buffer. This treatment also removes the insoluble protein aggregates that

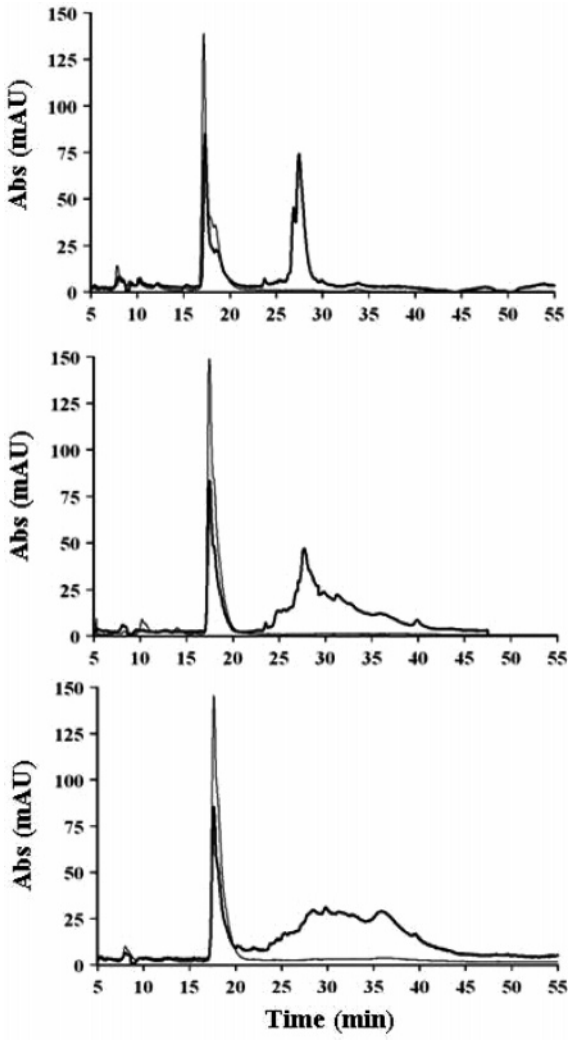

Figure 1. Reverse-phase HPLC analysis of hMb after reaction with 3-fluorophenol (molar ratio 1:15) and mushroom tyrosinase in 10 mM phosphate buffer, pH 7.4: (a, top) unreacted hMb, (b, middle) protein mixture after 4 h reaction time, and (c, bottom) after 24 h reaction time. The elution profile was monitored at the two wavelengths of 280 nm (bold trace) and 400 nm (thin trace). The trace detected at 280 nm was 4-fold increased in intensity.

slowly form at long reaction times. The reddish band that is collected contains a mixture of hMb and hMb−fQ adducts. The protein concentration was estimated by UV−vis spectroscopy, assuming that for the protein mixture $\epsilon_{410} = 150\ mM^{-1}\ cm^{-1}$ as for met-hMb. The spectra of the modified proteins confirm the presence of bound quinone residues as the low-energy tail of the heme Soret band contains a broad shoulder extending to about 500 nm. Regarding the formation of insoluble protein aggregates, their presence becomes visually detectable after several hours reaction time, but they may be contaminated by fQ polymerization products. The amount and rate of formation of these precipitates increases with tyrosinase concentration; for this reason the concentration of the enzyme was kept generally low in our experiments.

HPLC Analysis. The (soluble) protein components after reaction of hMb with 3-fluorophenol and tyrosinase at various reaction times were analyzed by reverse-phase HPLC. As shown in Figure 1a, the HPLC trace of a sample of native hMb contains two peaks because, due to the acidic conditions of the analysis, the free heme (peak at 17.9 min elution time) and the apoprotein (29.1 min) elute separately. Figures 1b and 1c show the HPLC chromatograms of samples of hMb after 4 and 24 h reaction

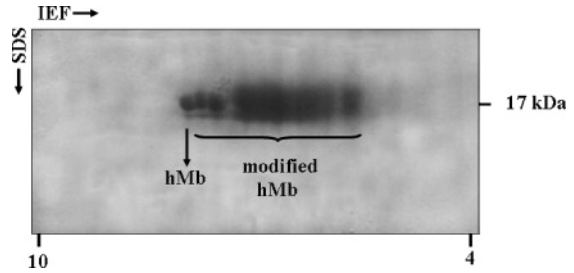

Figure 2. Two-dimensional and SDS-PAGE analysis of hMb after reaction with 3-fluorophenol and tyrosinase in 10 mM phosphate buffer, pH 7.4, after 4 h reaction time.

times, respectively, with 3-fluorophenol in the presence of tyrosinase. The reaction between hMb and reactive fQ clearly gives rise to a family of hMb−fQ adducts. The peak of apo-hMb strongly decreases in intensity and can hardly be distinguished under the envelope of overlapping peaks occurring between 25.0 and 40.0 min in the HPLC trace. The extent of protein modification increases with increasing reaction time, as is clearly shown by the complexity of the HPLC profile and the decrease in intensity of the peak corresponding to apo-hMb. In all cases, the chromatograms showed no appreciable differences in the heme elution time, thus suggesting that the prosthetic group is not affected by the reaction of the protein with fQs. Moreover, there was no evidence of the formation of heme−protein cross-linked species that could be induced by quinones or other reactive species, because no peak in the HPLC traces contained simultaneous absorption at 400 and 280 nm.

Two-Dimensional and SDS-PAGE Analysis. The presence of multiple peaks in the HPLC traces corresponding to hMb−fQ adducts was unraveled by two-dimensional and SDS-PAGE experiments. Several bands with different isoelectric points and different intensities were in fact observed in the two-dimensional polyacrylamide gel of the products of the reaction between hMb and fQ (Figure 2), in agreement with the HPLC data.

The comparison of the two-dimensional polyacrylamide gel of modified hMb's with that of wild-type hMb indicates that the hMb−fQ adducts are more acidic than hMb. Considering that the pH gradient used, from 4.0 to 10.0, is not linear, it is only possible to estimate from the spots of the hMb−fQ adducts that the covalent modification induces a shift of pI from 0.2 to 2.0 units from the 7.2 value of hMb.[45] The increased acidity of the modified protein can be accounted for on the basis of the reaction between reactive quinones and protein amino acids.

Protein Blotting Analysis. To identify the nature of the hMb modifications and to demonstrate that the quinones are covalently bound to hMb, a protein blotting analysis with NBT and Ponceau staining were performed. The NBT/glycinate staining enables the detection of the presence of quinoproteins because their interaction with NBT yields a blue-purple coloration.[54] The blotting analysis of the hMb−fQ adducts resulting from the reaction between hMb, 3-fluorophenol, and tyrosinase indeed showed the presence of a blue-purple coloration in correspondence with the hMb spot. Moreover, the gel revealed a blue-purple coloration in the region of high molecular weight proteins, probably corresponding to the formation of hMb oligomers. A further coloration with Ponceau stain, which specifically binds proteins, confirmed that the NBT stained bands are constituted by proteins.

Mass Spectrometry Analysis. To probe the modification of hMb by fQ residues, MS studies were performed. ESI-MS analysis of wild-type hMb indicated a molecular weight of 17 051 amu for the met protein, which agrees with the mass of 17 053 amu predicted from the amino acid sequence. MS

Table 1. Modification Sites of hMb by fQ Species Produced by Reaction of 3-Fluorophenol with Tyrosinase, as Obtained by HPLC/ESI-MS/MS Analysis

retention time (min)	peptide sequence[a]	peptide position	peptide mass[b]	mass increment[c]	percent modification[c]
29.8	G**H**PETLEKFDKFK	35−47	1683.8	108	78
35.1	**H**LKSEDEMKASEDLKK	48−63	1995.9	108	87
22.9	ASEDLKK**H**GATVLTALGGILKK	57−78	2358.3	108	64
32.5	GH**H**EAEIKPLAQSHATKHKIPVK	80−102	2664.2	108	84
45.5	GLSDGEWQLVLNVWGKVEADIPG**H**GQEVLIR	1−31	3630.4	216	24

[a] In bold is the histidine residue containing the modification. [b] In amu units. [c] With respect to the corresponding peptide of wild-type hMb.

analysis of the reaction solutions containing hMb−fQ adducts allowed the detection of, in addition to the peak for the unmodified protein, a series of peaks characterized by molecular weights higher than that of wild-type hMb. Among these, the peak of a larger relative intensity corresponded to the addition of a single fQ to the protein, while the other peaks corresponding to the addition of up to five monomeric fQ derivatives were progressively weaker as the molecular mass increased. No increase in molecular weight was detected for the heme prosthetic group separated from the apo-hMb derivatives.

HPLC-ESI-MS/MS Analysis. The characterization of the sites of fQ modification introduced into hMb was performed on samples of the reaction solution after 4 h of reaction time. To this end, the polypeptide fragments resulting from tryptic digestion of the apo-hMb protein mixture (unmodified and modified) were analyzed by HPLC-ESI-MS/MS. The data showed that five peptide fragments containing fQ modifications were present as bicharged ions with *m*/*z* 841.9 (mass of 1683.8 amu), *m*/*z* 998.5 (mass of 1995.9 amu), *m*/*z* 1180.1 (mass of 2358.3 amu), *m*/*z* 1333.1 (mass of 2664.2 amu), and *m*/*z* 1815.7 (mass of 3630.4 amu), respectively. They correspond to fQ-modified fragments 35−47 (containing H36), 48−63 (containing H48), 57−78 (containing H64), 80−102 (containing H81, H82, H93, and H97), and 1−31 (containing H24), respectively. The peptides with masses of 1683.8, 1995.9, 2358.3, and 3630.4 amu contain a chemical species with a mass increment of 108 amu with respect to the parent peptides, which is compatible with the addition of a monomeric fQ residue. The ion corresponding to 2664.2 amu shows a mass increment of 216 amu with respect to the parent peptide (Table 1), which could correspond to a covalently bound dimeric fQ species (resulting from the condensation between 3-fluoroquinone and one molecule of 3-fluorophenol).[37]

All fQ-modified peptides were analyzed by CID. The MS/MS spectrum of the fragment 57−78 is shown, as an example, in Figure 3, where the y and b ion series are reported. A mass difference of 108 amu was detected between b7 and b8 that allowed the unequivocal assignment of a fQ residue bound to H64.

A quantitative analysis of the five modified peptides was obtained by comparing, in the extracted ion chromatogram (EIC), the areas of the peaks corresponding to the five fQ-bound peptides (of masses 1683.8, 1995.9, 2358.3, 2664.4, and 3630.4 amu, respectively) with that of the corresponding peptides resulting from native hMb (of masses 1575.8, 1887.9, 2250.3, 2556.4, and 3414.4 amu, respectively). The retention times and percent modification of the five fQ-modified peptides are given in Table 1. The occurrence of modification at the cysteine residue C110 was also carefully investigated, but no appreciable modification was detected. Therefore, the peak corresponding to fQ modification at C110 was either absent or extremely weak (<1%) and hidden under the noise.

To clarify if the lack of modification at C110 was due to the inaccessibility of this residue, we performed an experiment using apo-hMb. Treatment of apo-hMb with fQ induced severe precipitation of the protein. Treatment of the (minor) portion of the modified apoprotein remaining in the solution with trypsin, followed by HPLC-MS/MS analysis of the peptide fragments, showed similar modifications as observed with holo-hMb. The extent of the modifications was not satisfactorily reproducible, probably due to the small amount of soluble protein, but the modification yields of the His residues were significantly higher with respect to the experiments performed with holo-hMb. It is worth noting that the tryptic peptides observed with modified apo-hMb covered the complete hMb sequence except for all of the peptides containing the C110 residue (to any detectable extent). Probably, when the Cys residue is exposed and accessible to fQ, its modification is complete and occurs with precipitation of the protein.

Circular Dichroism. A CD study was carried out to analyze the conformational changes undergone by hMb upon fQ modification. The far-UV CD spectra of solutions of the modified hMb at various reaction times show progressive changes with respect to that of the wild-type protein (Figure 4). The changes consist of a decrease in the intensity of the positive CD peak around 192 nm and the negative CD peak at 222 nm and of a small increase in the intensity of the negative CD peak at 208 nm. The variations in the far-UV CD spectrum clearly increase with the reaction time. The CD data were analyzed to evaluate the effect of the fQ modifications on the secondary structure content of hMb. An important observation is that the α-helix contribution decreased gradually with increasing reaction time, from 80.6% (calculated for native hMb using the Jasco software) to 76.6% for the mixture containing hMb−fQ adducts after a reaction time of 2 h and to 73.9% for that obtained after 4 h. In contrast, the random contribution to secondary structure increased with increasing reaction time (from 18.5% in native hMb to 23.4% and 26.1% after 2 and 4 h reaction times, respectively).

Fluorine NMR Experiments. As it is known from our previous study on the tyrosinase oxidation of fluorophenols,[37] inorganic fluoride is released upon reaction of the fQ primary product. The reaction of hMb with 3-fluorophenol and tyrosinase was therefore followed by ^{19}F NMR to confirm the production of fluoride ion as a side product of the reactions of fQ species with protein residues and 3-fluorophenol. Blank experiments carried out in the same conditions as for hMb derivatization but in the absence of hMb allowed the estimation of the amount of inorganic fluoride produced in the competitive 3-fluorophenol oxidative polymerization catalyzed by tyrosinase. To determine reliable amounts of fluoride, these experiments had to be carried out using concentrations of hMb and fluorophenol in the millimolar range. Therefore, the concentrations of all reagents were increased about 100-fold with respect to those used in the

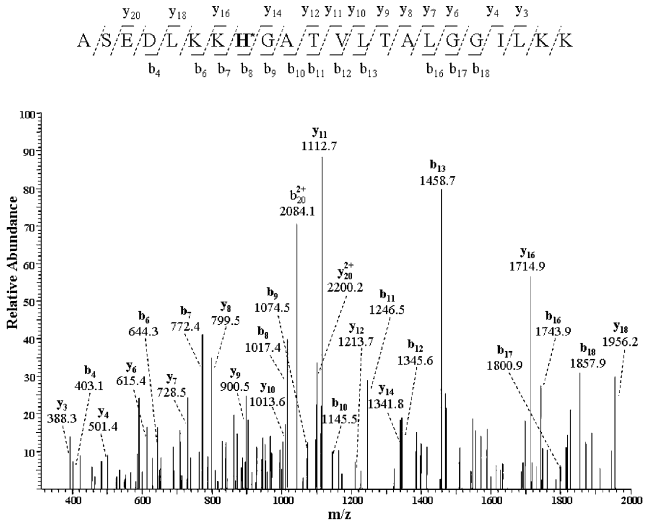

Figure 3. MS/MS spectrum of the *m*/*z* 1180.1 peak (mass of 2358.3 amu) assigned to the 57−78 peptide in a singly charged state and containing as a single modification the fluorocatechol adduct at H64. The assignment of the y and b ion series is shown.

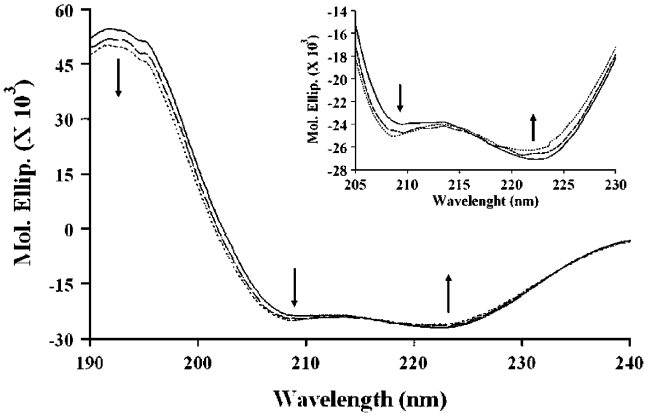

Figure 4. Far-UV CD spectra (190−240 nm) of native and modified hMb's. Control hMb (continuous trace) and hMb (0.1 mM) reacted with 3-fluorophenol (in a molar ratio of 1:15) and tyrosinase (50 nM) after reaction times of 2 h (dashed trace) and 4 h (dotted trace). Measurements were performed in 10 mM phosphate buffer, pH 7.4, at 25 °C, using a 1 mm path length cell.

HPLC experiments described above. This caused an obvious increase in the rates of all of the processes involved but allowed us to monitor the competitive effect of hMb on the evolution of the enzyme-generated fluoroquinone. As shown in Figure 5, inorganic fluoride is continuously produced in the enzymatic oxidation of 3-fluorophenol in the absence of hMB, until after approximately 30 min tyrosinase becomes completely inactivated by the various oligomeric quinone species formed in the reaction conditions. Fluoride is generated here through the formation of the addition product between 3-fluorophenol and the primary fQ species, whereas further oligomerization of this adduct occurs without the production of fluoride.[37] When hMb is present, the protein nucleophilic residues compete with 3-fluorophenol in the reaction with fQ, and this process also produces fluoride. Though, in the presence of hMb, the amount of fluoride is lower than that produced in its absence, indicating that the protein residues react easily not only with monomeric fQ, which would result in a complete release of fluoride (Scheme 1), but also with the oligomeric fQ species resulting from the quinone polymerization process. This is confirmed by the modification of H24 with a dimeric fluoroquinone derivative found under much milder reaction conditions (Table 1), while

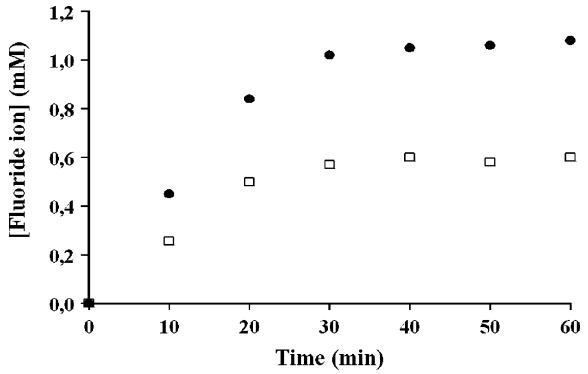

Figure 5. Time progress of the production of inorganic fluoride by enzymatic oxidation of 3-fluorophenol in the absence (●) and in the presence (□) of native hMb.

a more extensive protein modification with oligomeric quinone derivatives is expected in the conditions of the NMR experiment, where a 100-fold higher concentration of the reagents is employed.

Unfolding Experiments. To evaluate the stabilities of hMb−fQ derivatives, denaturation experiments were carried out with Gdn-HCl. Figure 6 illustrates the absorbance variations of the Soret band of samples of hMb after reaction with fQ, generated in the usual way (reaction times of 0, 4, 8, 24, and 48 h) and measured at equilibrium in the presence of different concentrations of Gdn-HCl. A major sharp transition is observed between 1.0 and 2.0 M Gdn-HCl for wild-type hMb, but the beginning of this transition occurs at progressively smaller Gdn-HCl concentrations as the extent of fQ modification of the protein increases. Denaturation is reversible, as shown by dialyzing out Gdn-HCl from the solution. The data on the stability of the hMb−fQ adducts in the presence of Gdn-HCl were analyzed assuming a simple two-state model; the values of the unfolding midpoint [D_0] for the proteins at various stages of fQ derivatization are reported in Table 2. The data were subsequently used to calculate ΔG°_{obs}, the Gibbs energy of unfolding, at each denaturant concentration. From the replots of ΔG°_{obs} versus [Gdn-HCl] it was possible to evaluate ΔG°_{N-U}, the Gibbs energy change at zero denaturant concentration, by extrapolation of the resulting linear plots and the $-m$ values from the slope. The Gibbs energies calculated for the conversion of the proteins from the native to the unfolded state are all positive (Table 2), indicating that the denaturation is a nonspontaneous, unfavorable process. Finally, the $-m$ parameter (Table 2) shows a clear dependence on the extent of fQ modification, as expected for an unfolding process involving an increase in the solvent-exposed surface area of the protein (see inset of Figure 6).

Congo Red Spectrophotometric Assay. Congo Red is used as a spectrophotometric reagent for the identification of amyloid fibrils in samples in vitro.[55] The interaction between Congo Red and amyloid fibrils develops a characteristic optical band at 540 nm. The UV−vis spectroscopic assay for fQ-modified hMb shows the slow appearance of the band at 540 nm, indicative of the possible presence of fibrillar aggregates in solution. The absorption band appears a few minutes after adding the dye to the solution of fQ-modified hMb; the band increases in intensity for about 45 min and then remains constant. Even though the Congo Red assay is one of the most widespread methods for the identification of amyloid fibrils, it is not suitable to quantify the amount of fibrils present in solution because the dye interacts with the fibrils by different mechanisms depending on the component peptide.[55] Moreover, it has been recently demonstrated that Congo Red can bind to a large number of proteins

Scheme 1. Proposed Reaction Mechanism between Tyrosinase-Derived fQ Species and hMb Histidine Residues

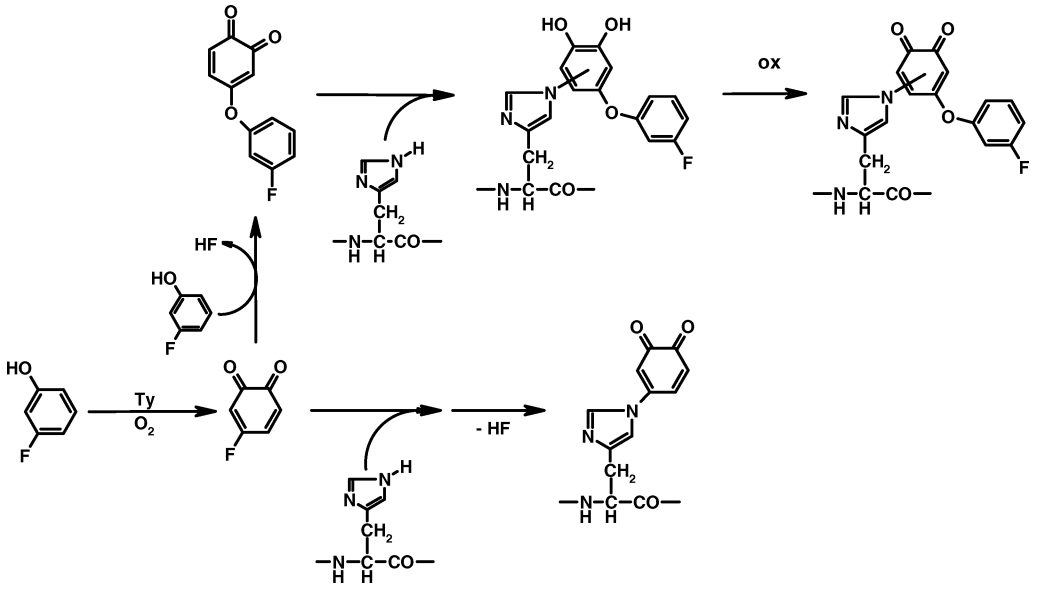

Table 2. Thermodynamic Data on Gdn-HCl-Induced Unfolding of hMb−fQ Derivatives

reaction time (h)	$[D_0]$ (M)	ΔG°_{N-U} (kcal mol^{-1})	$-m$ (kcal mol^{-1} M^{-1})
0	1.60 ± 0.01	5.05 ± 0.15	3.13 ± 0.08
4	1.44 ± 0.01	3.45 ± 0.08	2.43 ± 0.03
8	1.30 ± 0.01	3.02 ± 0.06	2.35 ± 0.04
48	0.99 ± 0.01	2.38 ± 0.08	2.38 ± 0.06

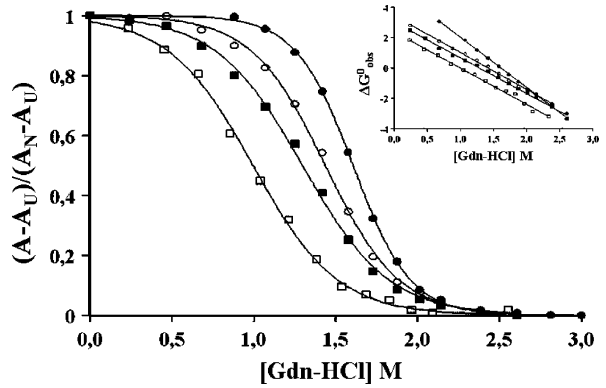

Figure 6. Equilibrium Gdn-HCl denaturation curves of the hMb−fQ adducts at different reaction times ((●) native HMb, (○) 4 h, (■) 8 h, (□) 48 h) at pH 6.8 and 25 °C monitored by absorbance variation of the Soret band of the protein. Data were normalized so that the absorbance value of 1.0 corresponds to the completely folded state of the proteins. The inset shows the linear plots of ΔG°_{obs} vs [Gdn-HCl] for the same samples.

in a nonspecific way[56] and that its binding efficiency is lower than that observed with other dyes.[57] To test for the possible interference with Congo Red by the other species present in the reaction mixture, four blanks containing native hMb, tyrosinase, 3-fluorophenol, and a mixture of hMb and tyrosinase were performed, but the UV−vis spectroscopic assays for all of blanks were negative, and no bands at 540 nm developed after the 45 min incubation time.

Congo Red Birefringence Assay. Birefringence upon staining with Congo Red is used as a method for the identification of amyloid fibrils. On polarization, the interaction between Congo Red and the amyloid fibrils develops apple-green birefringence. There was no substantial evidence that samples of fQ-modified hMb develop yellow-green birefringence.

Transmission Electron Microscopy. Although the structure of the insoluble aggregates of fQ-modified hMb formed at long reaction times was not a main objective of the present investigation, samples of protein solutions at relatively long reaction times, 24 and 48 h, were prepared for TEM observation. TEM analysis revealed that the samples were not homogeneous in that aggregates with different sizes and morphologies could be observed (Figure 7). Though, the majority of the aggregates consisted of oval structures, with a mean diameter of approximately 10 nm, and assemblies of these structures appeared to be organized in aggregates of larger sizes. The amount of these aggregates was connected to the extent of hMb derivatization and increased with reaction time. Clumps of amorphous material were also observed in all of the samples.

Discussion

The present study provides evidence that reactive quinone molecules induce multiple modifications of holo-hMb and, as a direct consequence, trigger unfolding and aggregation of the protein. hMb contains 19 Lys residues (accounting for about 12% of the total amino acids), 9 His (about 6%), and a unique cysteine residue, C110, that could easily undergo modification by reaction with quinones. Indeed, we recently found that hMb is much more reactive with RNS with respect to myoglobins from other sources because of the involvement of this Cys residue.[45] Thus, hMb is a good target for reactive quinone species.

Upon reaction of hMb with tyrosinase and 3-fluorophenol in mild conditions, an extensive modification of the protein by the fluoroquinones occurs, as indicated by HPLC and two-dimensional SDS-PAGE analysis. The modifications do not involve the heme cofactor; thus, the product of the reaction is a family of hMb derivatives containing modifications at amino acid residues (Figure 1) and having more acidic pI's with respect to the wild-type protein (Figure 2). The smear observed in the spots on two-dimensional SDS-PAGE clearly shows that the modifications affect the protein molecular weight, and the MS analysis on the hMb−fQ derivatives indicates that from one to five fQ residues have been added to the protein. In addition,

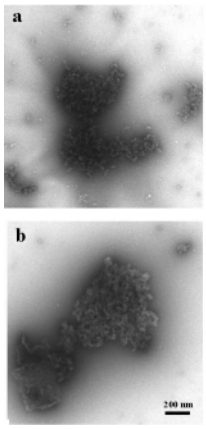

Figure 7. Morphology of hMb aggregates: (a) TEM images from sample of hMb after 24 h reaction time; (b) TEM images from the sample of hMb after 48 h of reaction time.

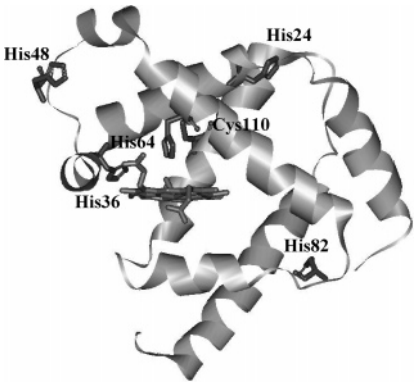

Figure 8. Computer-simulated three-dimensional structure of the hMb K45R/C110A mutant of human myoglobin in which the alanine residue A110 has been replaced with a cysteine residue by the Swiss-PdbViewer, version 3.7. The disposition of the side chains of H24, H36, H48, H64, and H82 as well as that of C110 are shown.

NBT staining of hMb−fQ species showed, besides the major ~17 kDa band corresponding to monomeric protein derivatives, traces of protein material at higher molecular weights, probably due to dimer and trimer protein oligomers. The small amount of these protein derivatives and their likely change in pI made apparently difficult their detection on the two-dimensional gel.

The HPLC-MS/MS analysis reveals that the main fQ modifications occurred at His residues 24, 36, 48, 64, and 82. The three-dimensional structure of wild-type hMb is not available. A reference structure for localizing the residues subjected to modifications is the crystal structure of the hMb K45R/C110A mutant.[58] Figure 8 reports a computer-simulated three-dimensional structure of the hMb K45R/C110A mutant in which A110 has been replaced with a cysteine residue by the Swiss-PdbViewer version 3.7. The disposition of the side chains of H24, H36, H48, H64, and H82 as well as that of C110 are shown. As is evident, apart from H64, all other histidine residues are on the protein surface and are clearly exposed to solvent. The significant derivatization undergone by H64 is thus surprising, as we have to take into account that H64 is in the distal cavity and should not be easily accessible. As it was postulated for the binding of O_2,[59] fluctuations of the protein backbone and the side chains can facilitate the binding process.[59] As proposed by Perutz and Matthews,[60] ligand migration from the heme pocket to the solvent, and vice versa, involves rotation of the side chain of the distal H64. The His-gate hypothesis was supported by crystallographic work on different myoglobins[61] and is now accepted on a firm basis due to extensive kinetic experiments carried out on Mb site-directed mutants. In fact, this local mobility makes possible the binding of ligands of the size of imidazole[62] to the heme iron and the access of simple phenols in the distal cavity.[63] We can thus assume that a similar mechanism enables the access of a fQ molecule, with size comparable to the above ligands, to the distal cavity.

In Scheme 1, the pattern of reactions undergone by the tyrosinase-generated fQ is shown. The quinone molecule can undergo a coupling reaction with excess 3-fluorophenol, to produce a dimeric fQ species,[37] or nucleophilic addition by the imidazole nucleus of histidine residues, both followed by HF elimination. It is interesting that in both cases the fluorine atom of the quinone directs the reaction, as inorganic fluoride is produced. The fQ dimer is subjected to a similar fate: further condensation with 3-fluorophenol or reaction with protein amino acid residues. In both cases, as the quinone ring is devoid of fluorine atoms, the reaction is a simple Michael addition that produces a catechol. The electron-rich catechol nucleus of this derivative undergoes easy oxidation to quinone by tyrosinase or, more likely, by redox exchange with other quinone species, as the mass increment (216 amu) detected for the modified peptide fragment corresponds to the fQ dimer derivative. However, the fQ-modified peptides are detected as the corresponding catechol derivatives (mass increment of 108 amu), likely because this quinone group undergoes reduction in the MS instrument. The quinone forms of the hMb−fQ adducts are in fact confirmed by their contribution to the optical spectra of the modified proteins and by the analysis with NBT staining. The yield of protein fQ modification depends, in any given reaction condition, on the competition between the reactions of fQ species with protein side chain residues and the coupling reactions with 3-fluorophenol and other oligomeric species that are responsible for polymer formation.[37] The latter reactions correspond to neuromelanin formation when the quinone species are produced from dopamine.[64] As shown by the fluorine NMR experiments, the protein nucleophilic residues react avidly with both monomeric fQ and the oligomeric fQ species produced by evolution of the primary fQ. This is confirmed by the detection of the fQ dimer modification of H24 characterized by MS analysis. This result is of particular importance for the biological reactions of dopamine quinone, because the evolution of this quinone is much faster than that of the fQ molecule studied here. Therefore, it is expected that protein modification by dopamine-derived species will involve not only monomeric DAQ but also the oligomeric quinone species formed on the way to DAQ melanization.

A further result that has an impact on the chemistry of protein covalent modification in vivo is the absence of any significant derivatization at C110, which is, at best, below the detectable limit of the analysis. The formation of protein 5-*S*-cysteinyl-dopamine or 5-*S*-cysteinyl-L-Dopa derivatives has been reported in the literature,[30,33,65] and indeed this amino acid is expected to be the most reactive toward quinones. For instance, the reactivity of *N*-acetylcysteine toward electrochemically generated DAQ is at least 10^6 times faster than that of *N*-acetylhistidine at neutral pH.[36,66] Though, quinones are sizable molecules and may not readily access buried residues. At the present stage, as no three-dimensional structure of hMb is available, we can thus speculate that C110 is not accessible to fluoroquinones (Figure 8) or, alternatively, that the fQ modification of the H64 residue in the neighborhood prevents its reaction with fQ. As expected, when the apoprotein is reacted with the fQ species under the same conditions, an extensive modification occurs, with almost complete aggregation and precipitation of

the protein. The cysteine residue, in particular, undergoes complete modification as after tryptic treatment of the small amount of protein remaining in the solution no peptides containing C110 were detected.

The most important consequence of fQ reactions with hMb residues is that, even with a moderate loss of secondary structure, the compact structure of holo-hMb becomes more easily unfolded and the protein tends to undergo aggregation. So far, the apo-form of skeletal muscle Mb has been reported to undergo structural change to a disordered structure and aggregation to amyloid fibrils,[43,44] but the conditions required for such a transformation were indeed harsh (pH 9, heating to 65 °C for days). Conversely, this study shows that quinone modification of holo-hMb leads to a loss of structure under mild conditions. The Gdn-HCl unfolding studies clearly show that fQ-modified hMb is progressively more susceptible to denaturation as the extent of fQ modification increases (Table 2). As quinone modification occurs at polar histidine residues, it is likely that this causes disruption of the hydrogen-bonding interactions established among the protein residues, and involving also the heme group, and thereby destabilizes the folding locally at the modification sites. This interpretation is confirmed by examination of the $-m$ values for hMb at various stages of fQ modification, which indicate that this modification progressively increases the surface area of the protein exposed to solvent. An indication of the local loss of secondary structure upon fQ modification of hMb has been obtained by the CD spectra, which clearly show that the reaction with fluoroquinones causes a concomitant loss in α-helix content with an increase in random coil content.

Solutions of fQ-modified hMb give a positive response to the Congo Red assay,[55] but the birefringence assay, which has a more stringent definition, excludes the presence of amyloid fibrils.[51] Although the analysis of the insoluble aggregates generated by fQ modification of hMb is outside the scope of the present investigation, TEM experiments show the presence of structured bodies of moderate size, probably corresponding to small oligomeric protofibrillar aggregates, but confirm the complete absence of fibrils. This is apparently in line with the results showing the effect of dopamine, which is known to promote aggregation of proteins[32] (likely through DAQ modification), but to prevent and even disaggregate amyloid fibrils.[31] In conclusion, we have shown here that modification of a moderate number of protein residues by quinone species has important effects even in the case of a protein with a globular, compact structure such as hMb. Post-translational protein modifications may as well trigger the onset of sporadic misfolding diseases. Studies on the consequences of protein−quinone adduct formation will contribute further to our understanding of the origins and development of neurological conditions related to Parkinson's disease.

Acknowledgment. This work was supported by grants from the Progetti di Ricera di Interesse Nazionale and Fondo degli Investimenti della Ricera di Base projects of the Italian Ministero dell' Instruzione, dell' Università, e della Recera. The authors thank Stefania Nicolis for preparing the sample of human myoglobin, Vittorio Bellotti (Department of Biochemistry, University of Pavia) for the polarized light microscopy experiments, and Luigi Bubacco (Department of Biology, University of Padova) for the TEM experiments.

References and Notes

(1) Halliwell, B. *J. Neurochem.* **2006**, *97*, 1634−1658.
(2) Ross, C. A.; Poirier, M. A. *Nat. Med.* **2004**, *10*, S10−S17.
(3) Ischiropoulos, H.; Beckman, J. S. *J. Clin. Invest.* **2003**, *111*, 163−169.
(4) Turko, I. V.; Murad, F. *Pharmacol. Rev.* **2002**, *54*, 619−634.
(5) Glaser, C. B.; Yamin, G.; Uversky, V. N.; Fink, A. L. *Biochim. Biophys. Acta* **2005**, *1703*, 157−169.
(6) Gibson, B. W. *Int. J. Biochem. Cell Biol.* **2005**, *37*, 927−934.
(7) Winklhofer, K. F.; Henn, I. H.; Kay-Jackson, P. C.; Heller, U.; Tatzelt, J. *J. Biol. Chem.* **2003**, *278*, 47199−47208.
(8) Souza, J. M.; Giasson, B. I.; Chen, Q.; Lee, V. M.; Ischiropoulos, H. *J. Biol. Chem.* **2000**, *275*, 18344−18349.
(9) Kim, K. S.; Choi, S. Y.; Kwon, H. Y.; Won, M. H.; Kang, T.-C.; Kang, J. H. *Biochimie* **2002**, *84*, 625−631.
(10) Krishnan, S.; Chi, E. Y.; Wood, S. J.; Kendrick, B. S.; Li, C.; Garzon-Rodriguez, W.; Wypych, J.; Randolph, T. W.; Narhi, L. O.; Biere, A. L.; Citron, M.; Carpenter, J. F. *Biochemistry* **2003**, *42*, 829−837.
(11) Reynolds, M. R.; Berry, R. W.; Binder, L. I. *Biochemistry* **2005**, *44*, 1690−1700.
(12) Casoni, F.; Basso, M.; Masignan, T.; Gianazza, E.; Cheroni, C.; Salmona, M.; Bendotti, C.; Sonetto, V. *J. Biol. Chem.* **2005**, *280*, 16295−16304.
(13) Radi, R. *Proc. Natl. Acad. Sci. U.S.A.* **2004**, *101*, 4003−4008.
(14) Dremina, E. S.; Sharov, V. S.; Schöneich, C. *J. Neurochem.* **2005**, *93*, 1262−1271.
(15) Hodara, R.; Norris, E. H.; Giasson, B. I.; Mishizen-Eberz, A. J.; Lynch, D. R.; Lee, V. M.-Y.; Ischiropoulos, H. *J. Biol. Chem.* **2004**, *279*, 47746−47753.
(16) Mishizen-Eberz, A. J.; Norris, E. H.; Giasson, B. I.; Hodara, R.; Ischiropoulos, H.; Lee, V. M.-Y.; Trojanowski, J. Q.; Lynch, D. R. *Biochemistry* **2005**, *44*, 7818−7829.
(17) Dean, R. T.; Dunlop, R.; Hume, P.; Rodgers, K. J. *Biochem. Soc. Symp.* **2003**, *70*, 135−146.
(18) Lashuel, H. A.; Hartley, D.; Petre, B. M.; Walz, T.; Lansbury, P. T. *Nature* **2002**, *418*, 291.
(19) Orr, H. T. *Nature* **2004**, *431*, 747−748.
(20) Stokes, A. H.; Hastings, T. G.; Vrana, K. E. *J. Neurosci. Res.* **1999**, *55*, 659−665.
(21) Asanuma, M.; Miyazaki, I.; Ogawa, N. *Neurotoxic. Res.* **2003**, *5*, 165−176.
(22) Sulzer, D.; Bogulavsky, J.; Larsen, K. E.; Behr, G.; Karatekin, E.; Kleinman, M. H.; Turro, N.; Krantz, D.; Edwards, R. H.; Greene, L. A.; Zecca, L. *Proc. Natl. Acad. Sci. U.S.A.* **2000**, *97*, 11869−11874.
(23) Lotharius, J.; Brundin, P. *Nat. Rev. Neurosci.* **2002**, *3*, 932−942.
(24) Wersinger, C.; Sidhu, A. *Neurosci. Lett.* **2003**, *342*, 124−128.
(25) Lotharius, J.; Brundin, P. *Hum. Mol. Genet.* **2002**, *11*, 2395−2407.
(26) Moussa, C. E.-H.; Wersinger, C.; Tomita, Y.; Sidhu, A. *Biochemistry* **2004**, *43*, 5539−5550.
(27) Conway, K. A.; Rochet, J.-C.; Bieganski, R. M.; Lansbury, P. T., Jr. *Science* **2001**, *294*, 1346−1349.
(28) Whitehead, R. E.; Ferrer, J. V.; Javitch, J. A.; Justice, J. B. *J. Neurochem.* **2001**, *76*, 1242−1251.
(29) Xu, Y.; Stokes, A. H.; Roskoski, R., Jr.; Vrana, K. E. *J. Neurosci. Res.* **1998**, *54*, 691−698.
(30) LaVoie, M. J.; Ostaszewski, B. L.; Weihofen, A.; Schlossmacher, M. G.; Selkoe, D. J. *Nat. Med.* **2005**, *11*, 1214−1221.
(31) Li, J.; Zhu, M.; Manning-Bog, A. B.; Di Monte, D. A.; Fink, A. L. *FASEB J.* **2004**, *18*, 962−964.
(32) Cappai, R.; Leck, S.-L.; Tew, D. J.; Williamson, N. A.; Smith, D. P.; Galatis, D.; Sharples, R. A.; Curtain, C. C.; Ali, F. E.; Cherny, R. A.; Culvenor, J. G.; Bottomley, S. P.; Masters, C. L.; Barnham, K. J.; Hill, A. F. *FASEB J.* **2005**, *19*, 1377−1379.
(33) Rodgers, K. J.; Hume, P. M.; Morris, J. G. L.; Dean, R. T. *J. Neurochem.* **2006**, *98*, 1061−1067.
(34) Rodgers, K. J.; Dean, R. T. *Int. J. Biochem. Cell Biol.* **2000**, *32*, 94−955.
(35) Rodgers, K. J.; Hume, P. M.; Dunlop, R. A.; Dean, R. T. *Free Radical Biol. Med.* **2004**, *37*, 1756−1764.
(36) Xu, R.; Huang, X.; Kramer, K. J.; Hawley, M. D. *Bioorg. Chem.* **1996**, *24*, 110−126.
(37) Battaini, G.; Monzani, E.; Casella, L.; Lonardi, E.; Tepper, A. W. J. W.; Canters, G. W.; Bubacco, L. *J. Biol. Chem.* **2002**, *277*, 44606−44612.
(38) Sanchez-Ferrer, A.; Rodriguez-Lopez, J. N.; Garcia-Canovas, F.; Garcia-Carmona, F. *Biochim. Biophys. Acta* **1995**, *1247*, 1−11.
(39) Xu, Y.; Stokes, A. H.; Freeman, W. M.; Kumer, S. C.; Vogt, B. A.; Vrana, K. E. *Mol. Brain Res.* **1997**, *45*, 159−162.
(40) Everse, J.; Coates, P. *Free Radical Biol. Med.* **2004**, *37*, 839−849.
(41) Hastings, T. G. *J. Neurochem.* **1995**, *64*, 919−924.
(42) Thomas, D. M.; Francescutti-Verbeem, D. M.; Kuhn, D. M. *FASEB J.* **2006**, *20*, 515−517.

(43) Fändrich, M.; Flechter, M. A.; Dobson, C. M. *Nature* **2001**, *410*, 165−166.
(44) Fändrich, M.; Forge, V.; Buder, K.; Kittler, M.; Dobson, C. M.; Diekmann, S. *Proc. Natl. Acad. Sci. U.S.A.* **2003**, *100*, 15463−15468.
(45) Nicolis, S.; Pennati, A.; Perani, E.; Monzani, E.; Sanangelantoni, A. M.; Casella, L. *Chem.—Eur. J.* **2006**, *12*, 749−757.
(46) Duckworth, H. W.; Coleman J. E. *J. Biol. Chem.* **1970**, *245*, 1613−1625.
(47) Gianazza, E.; Astrua-Testori, S.; Giacon, P.; Righetti, P. G. *Electrophoresis* **1985**, *6*, 332−339.
(48) Laemmli, U. K. *Nature* **1970**, *227*, 680−685.
(49) Antonini, E.; Brunori, M. *Hemoglobin and Myoglobin in Their Reactions with Ligands*; North Holland Publishing: Amsterdam, 1971.
(50) Choi, J.; Terazima, M. *J. Phys. Chem. B* **2002**, *106*, 6587−6593.
(51) Westermark, P. *FEBS J.* **2005**, *272*, 5942−5949.
(52) Puchtler, H.; Sweat, F.; Levine, M. *J. Histochem. Cytochem.* **1962**, *10*, 355−364.
(53) Varadarajan, R.; Lambright, D. G.; Boxer, S. G. *Biochemistry* **1989**, *28*, 3771−3781.
(54) Paz, M. A.; Flückiger, R.; Boak, A.; Kagan, H. M.; Gallop, P. M. *J. Biol. Chem.* **1991**, *266*, 689−692.
(55) Nilsson, M. R. *Methods* **2004**, *34*, 151−160.
(56) Eisert, R.; Felan, L.; Brown, L. R. *Anal. Biochem.* **2006**, *353*, 144−146.
(57) Sabaté, R; Esterlrich, L. *Biopolymers* **2003**, *72*, 455−463.
(58) Hubbard, S. R.; Hendrickson, W. A.; Lambright, D. G.; Boxer, S. G. *J. Mol. Biol.* **1990**, *213*, 215−218.
(59) Brunori, M.; Gibson, Q. H. *EMBO Rep.* **2001**, *2*, 674−679.
(60) Perutz, M. F.; Matthews, F. S. *J. Mol. Biol.* **1966**, *21*, 199−207.
(61) Bolognesi, M.; Cannillo, E.; Ascenzi, P.; Giacometti, G. M.; Merli, A.; Brunori, M. *J. Mol. Biol.* **1982**, *158*, 305−315.
(62) Monzani, E.; Alzuet, G.; Casella, L.; Redaelli, C.; Bassani, C.; Sanangelantoni, A. M.; Gullotti, M.; De Gioia, L.; Santagostini, L.; Chillemi, F. *Biochemistry* **2000**, *31*, 9571−9582.
(63) Redaelli, C.; Monzani, E.; Santagostini, L.; Casella, L.; Sanangelantoni, A. M.; Pierattelli, R.; Banci, L. *ChemBioChem* **2002**, *3*, 226−233.
(64) Zucca, F. A.; Giaveri, G.; Gallorini, M.; Albertini, A.; Toscani, M.; Pezzoli, G.; Lucius, R.; Wilms, H.; Sulzer, D.; Ito, S.; Wakamatsu, K.; Zecca, L. *Pigm. Cell Res.* **2004**, *17*, 610−617.
(65) Whitehead, R. E.; Ferrer, J. V.; Javitch, J. A.; Justice, J. B. *J. Neurochem.* **2001**, *76*, 1242−1251.
(66) Xu, R.; Huang, X.; Morgan, T. D.; Prakash, O.; Kramer, K. J.; Hawley, M. D. *Arch. Biochem. Biophys.* **1996**, *329*, 56−64.

BM070409H